Paper No. 035

Experimental Bench Testing of an Active-Twist Rotor

Johannes Riemenschneider*, Ralf Keimer*, Steffen Kalow*,

*Institute of Composite Structures and Adaptive Systems, Lilienthalplatz 7, 38108 Braunschweig, Germany

Johannes.Riemenschneider@dlr.de

Abstract

Model rotor blades are needed to validate numerical models and simulation tools. In order to do so, a proper characterization of the model rotor blades is urgently needed. Over the years a set of techniques was developed to characterize properties of active twist blades. Most of the methods can be applied to standard passive blades as well. Active twist rotor blades have been developed for the use in secondary rotor control such as higher harmonic control (HHC) and individual blade control (IBC). The basic principle of such blades is the implementation of piezoelectric actuators into the blades, using different types of coupling, causing the blades to twist. At the DLR model scale blades have been manufactured to demonstrate the feasibility of such systems. This paper is describing the experimental characterization methods for active twist blades. Both the elastic and mass related properties are discussed as well as the actuation behavior - especially for very low frequencies.

1 Principles of Active Twist

The basic principle of individual blade control and its benefits for an improved aerodynamic behavior has been shown in many different studies [1]. The goals are vibration reduction, noise reduction and performance improvement. One concept which has been investigated in detail is active twist. For several years the German Aerospace Center (DLR) has been investigating this technology and built several model rotor blades. A history of these activities can be found in [2, 3, 4]. The basic principle of this technology are skin integrated patch type actuators to introduce shear strain into the skin. Piezoceramic d_{33} actuators can be used for such purposes. The commercially available Macro Fiber Composites (MFC, see figure 1) were used for the DLR blades. Also the dynamics needed to excite a blade at frequencies up to 100 Hz is given by these actuators. Due to the use of the d_{33}-Effect these actuators show strains of up to 1600μm/m. With the given electrode spacing of the MFCs voltages up to 1500V are necessary to yield these active strains. The design of the skin can be optimized in order to maximize the twist angle, the twist momentum or the twist work (see also [5]). The relation between the momentum M, the twist rate θ' and the torsional rigidity GI is given by the following equation.

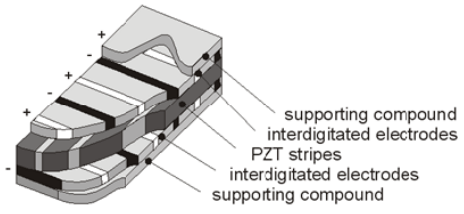

Figure 1: Piezoceramic actuator using the d_{33}-Effect: MFC by NASA.

$$M = \theta' \cdot GI$$

2 STAR blades

The star blades, which build a complete model rotor built by DLR can be seen in Figure 2. For identification the individual blades are named by letters from the Greek alphabet (α, β, γ, δ, ε). Most of the characterization techniques described in this paper will be demonstrated with values from these blades. The geometry is based on a Mach scaled BO 105 model blade with a radius of 2 m. The blades are optimized for maximum twist momentum. The GFRP skin is assembled of unidirectional plies at an angle of $\pm 45°$. The actuation system of the blades is composed of 24 Macro Fiber Composite actuators that are integrated in the upper

Figure 2: ActiveTwist blade set

and lower skin of the blade (see Figure 2).

The working direction of the actuators is in 45° with respect to blade axis. Hence strain is induced in the main strain direction of torsion deformation and forces the blade to twist. To have a maximum in control flexibility the blade itself is wired in a way that allows to operate several actuator segments individually. The tests described in this document are carried out in a non-rotating system. The goal is to determine the following parameters:

- Flap-bending stiffness
- Torsional stiffness
- Location of elastic axis
- Active twist for very low frequencies
- Nonlinearity of active twist

3 Mechanical Properties

Stiffness measurements were carried out using the fact that all investigated blades show constant cross section set ups over a certain span, in which the properties do not change. A clamping condition was chosen, which allows the blade to be loaded like a single side supported beam. Resulting deflections at the free end of the blade were used to derive the stiffness properties in the considered region. Major issue is the clamping condition, which consists of a clamp shaped as the blades airfoil in the region of the actuator closest to the root. In order to make the boundary condition even more rigid, the blade root itself was also clamped to the test rig in the rigion of the bolts. That way any bending that might occur in the clamping region was minimized. This is important to allow simple beam theory to be applied.

3.1 Applying Forces

Mechanical properties of the rotor-blades are determined for the part with uniform cross-section, only. Clamping is carried out as described above. To determine torsional stiffness, flap-bending stiffness and elastic axis external forces are used to deform the rotor-blade. Load introduced for bending is a dynamic force introduced through a string and pulled by an excenter rotating with 0.3 Hz. The force is applied to a lever (which extends in chord direction) at the tip of the rotor blade. It is ensured that the vector of the force is perpendicular to the lever. The use of this dynamic force ensures a constant time history in order to avoid creeping effects of the glass-fiber-composite material of the rotor-blade. The standard procedure is to apply the load at different positions along the lever, such as -300 mm, -150 mm, 0 mm, +150 mm, +400 mm - 0 mm corresponding to leading edge, positive sign in direction to trailing edge. The dynamic forces show approximately 6 N amplitude peak-peak with different offsets.

3.2 Measuring Displacements

Displacements at the blade-tip are measured with a photogrammetric system. The clamp is equipped with a stochastic black-white pattern (see Figure 3). It is attached to the blade in parallel to the chord of the profile. The coordinate-system of the measurement is transposed to this clamp in a way that X is oriented cord-wise, Y is oriented in flap direction and Z is parallel to the blades axis. A lever attached to the clamp is used to apply forces in Y-direction to the blade tip (see Figure 3 above the clamp). By applying forces at different positions of the lever the elastic axis can be determined. An example of the measured displacements in Y-direction is displayed in Figure 4. The change in displacement over chord is a clear indicator for an in-plain rotation of the section. Depending on the distance between the load application position and the elastic axis, there is a rotary displacement in the section. Linear interpolation will help to find the exact position of the elastic axis in chord wise direction. Loading in this location will result lead to

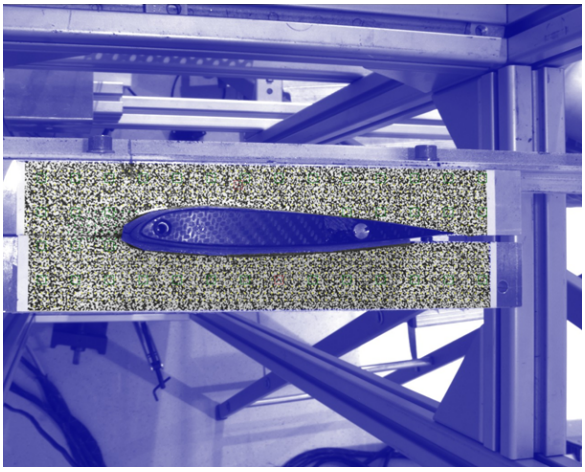

Figure 3: Blade-Tip with attached clamp

pure bending without any torsion. Once the elastic axis in found, the blade will be loaded by a single bending load $F(t)$ in this position, only. Resulting bending displacements dy are measured. Using linear beam theory the bending stiffness EI is calculated using these displacements and forces and the distance l between the clamp and the load introduction.

$$EI = \frac{F \cdot l^3}{3 \cdot dy} \tag{1}$$

Measurements for torsion regidity GI use loading by a momentum about the elastic axis. In order to evaluate the result the angle of the displacement φ and the torsion moment M_t is needed. The moment can be introduced by different means, either as a pair of forces around an axis or by a single force. For measurements with single forces the distance between the elastic axis and the load introduction is measured. Together with the applied forces the moment can be derived. Relating the calculated moment to the tip twist angles gives the torsional stiffness by the linear equations.

$$GI = \frac{M_t \cdot l}{\varphi} \tag{2}$$

This method was validated with calculations using the DLR cross section analysis routine. A prerequisite for accurate measurements is a long enough distance l between clamping and load introduction location. That way the influence of the imperfect clamping condition is minimized. A length of 10 times chord was shown to be sufficient.

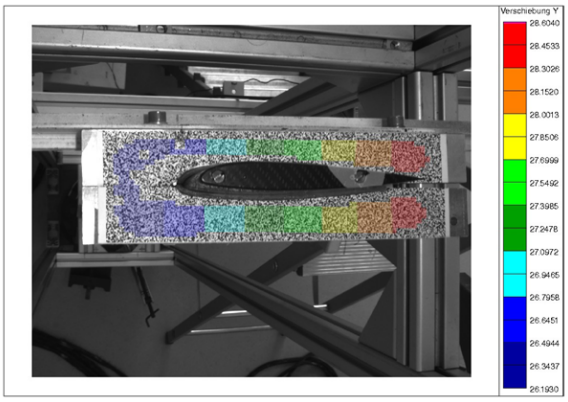

Figure 4: Result of Photogrammetric System, Displacement in Y-Direction

3.3 Example Results

As an example the experimental data for all STAR blades are given in the following paragraph. At first the location of the elastic axis was determined for all five blades as seen in Figure 5. It can

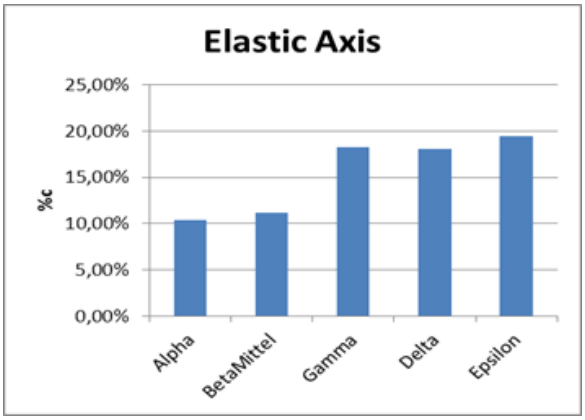

Figure 5: Elastic Achsis of STAR blades

clearly be seen, that there is a strong difference between blade alpha, beta and the other three blades. Those two blades are the highly instrumented ones. This difference is caused by the additional wires, that are applied to connect all sensors. Even though dummy wires have been used in the other blades, the stiffness could not be matched exact enough. In the next step the bending stiffness was determined. At first the standard deviation of the measurement itself was investigated. The technique was applied three times for the same blade. In between the measurements the complete setup was disassembled. The result

of the three measurements can be found in Figure 18. The standarddeviation is as low as 1.2%. That means that the technique is quite robust regarding experimental tolerances. As a result all blades were measured for their flap stiffness shown in Figure 6.

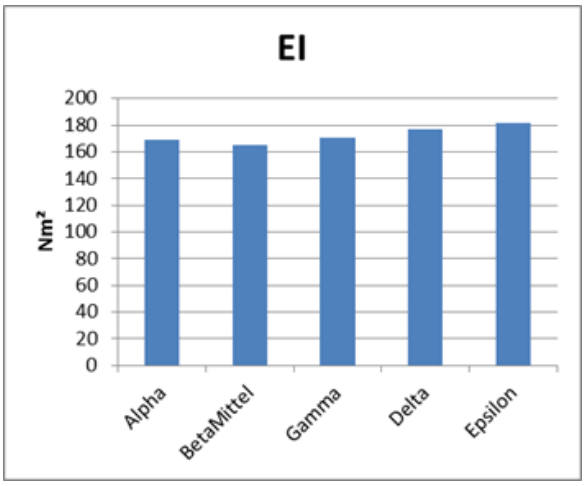

Figure 6: Flap Bending Stiffness of STAR blades

The standard deviation is in the order of 3 %. This shows, that the blades are built with rather similar flap stiffness.

4 Geometric properties

The outer geometry of the blades is an essential parameter for the aerodynamic performance of any rotor blade. For the validation of any wind tunnel experiment it is fundamental to know the built airfoil shape rather than the designed shape. Also it is good to know the accuracy of the manufacturing technique, especially if its newly developed especially for the given blades. This is why special measures were taken to analyze the built shape. The technique used is the optical 3D Scanner ATOS by GOM, using photogrammetric techniques with pattern projection to scan the surface of the blade. Both stripe patterns as well as phase shifted intensity variations are used by the system. Since the blade could not be measured in one single scan in the appropriate resolution, the TRITOP system also by GOM was used, to rearrange several scans to one overall dataset. As a result a cloud of points is available, which can be further analyzed. Two properties were tested: airfoil accuracy and twist distribution. In Figure 7 the distances between the design and the measured contour in plotted for radial position 50% and 80% for blade ε.

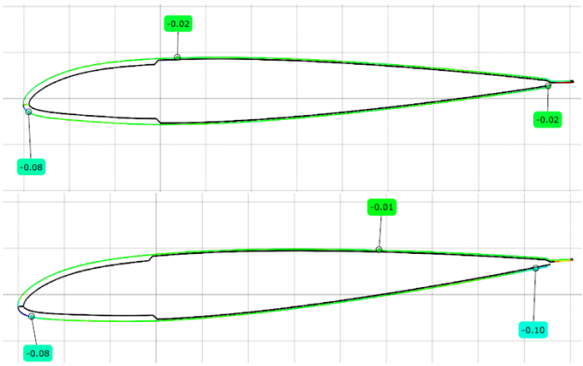

Figure 7: Comparison of a hardware scan with the design profile - given values are in mm, radial position 50% and 80%

The differences between the designed air foils and the built geometries was given for those sections by under 0.02 mm, which is a deviation of much less of one percent of the profile thickness. These values are in the region of the accuracy of the scan resolutions. The method seems to be appropriate to be applied for such analysis. In order to measure the twist distribution of the blade, several sections like the ones shown have been generated and a center line is created in each of them. The relative angle of these lines is compared as the twist distribution of the blade.

5 Mass related properties

The concept used to identify the mass distribution for a rotor blade is described in [6]. The basic idea of this method is the volumetric computer tomographic scan of the complete blade including details as foam, skin, cables etc. Differences between blades can be seen simply by post processing the CT-data. Figure 8 shows two different blades with different inner designs, which can be easiely evaluated by CT. This method offers the characterization of mass per span and inertias of a given cross section. In addition, for the STAR blades just a simple measurement of the blade weight and the span wise position of the cg was carried out. Figures 9 and 10 show the results of such measurements for the unbalanced blades just after completing the GFRP structure. This method is valid to find blade to blade differences in order to plan blade balancing.

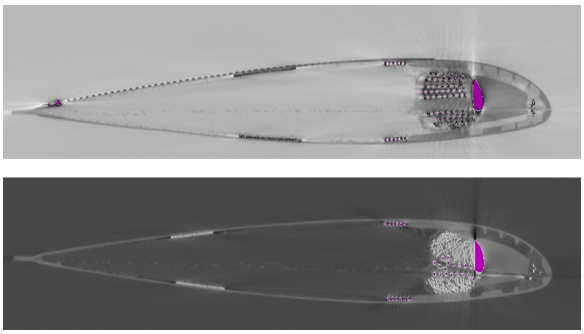

Figure 8: CT of different bladesshowing differences in inner structural designs

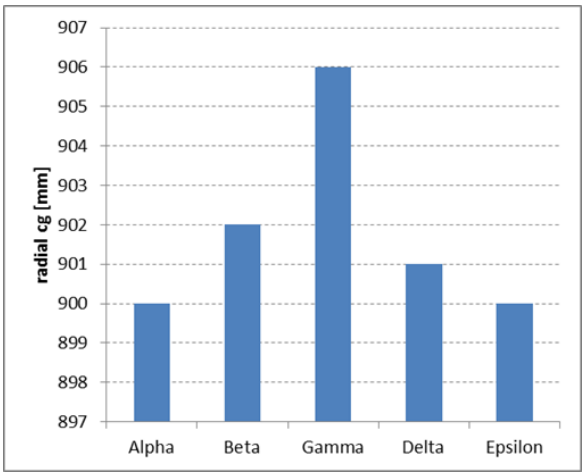

Figure 9: cg in radial direction after production - before additional balancing

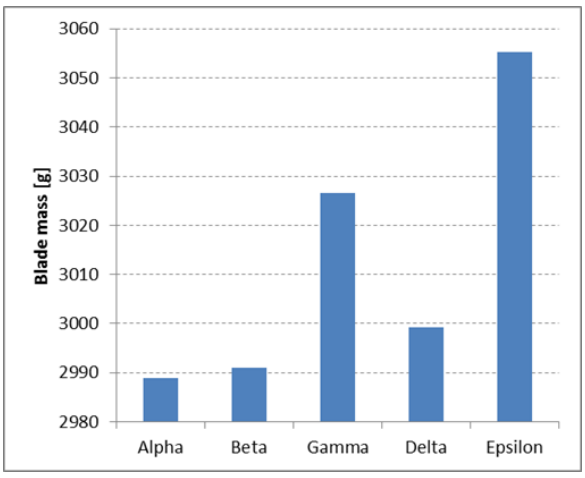

Figure 10: Mass of the STAR blades

6 ACTUATION

The twist actuation of the blades is a crucial examination for any active twist blade. In a lab test there are different ways to measure the displacements resulting from the twist actuation. One way to measure the twist is the same that was used to derive the bending and torsion stiffness, using a stereo camera system to derive displacements of the blade tip resulting from the actuation.

6.1 standard actuation test

As a standard the piezoceramic actuators were loaded with an electrical amplitude of -500V to +700V with a frequency of 0.01 Hz. The resulting active twist was measured at the blade tip. In order to test the system for repeatability the STAR blade Beta was measured three times with a complete disassembly of the testing setup in between. It could be shown, that the repeatability is rather

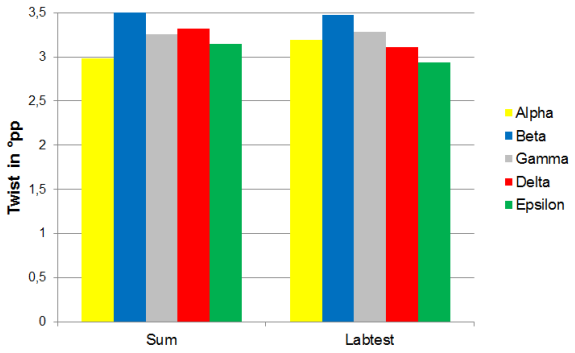

Figure 11: Twist actuation with individual excitation of each segment and collective actuation of all actuators

good (see Figure 19). Following this measurement the active twist performance of all STAR blades was measured (see Figure11). This was done in two different ways: once all actuators were loaded at the same time and once the actuators were activated segment by segment. There is no clear trend, of which configuration is producing higher overall twist. The method itself gives a good indication of the blade to blade differences.

In order to get a feeling of the nonlinearities of the actuation, additional tests were carried out, investigating the influence of different DC voltage offsets, amplitudes and different very low frequen-

cies. These experiments were carried out with just a few actuator segments of the AT4 blades by DLR. Since the measurements were about twist only, the flap and lag deflections were constrained by a support in the elastic axis. The tip twist deflections were measured with a single laser at the trailing edge. That way real time analog measurement was possible.

6.2 Influence of DC voltage offset

At first the electrical offset to drive the active twist was changed at a fixed amplitude of +/- 200V and a frequency of 1Hz. The results in Figure 12 indicate, that for offsets in the middle of the operating range the amplitudes are slightly higher than for those above and below. The trend is not really strong, but it is in agreement with the slope of a standard hysteresis of a piezoceramic actuator, where the highest slopes are found for medium actuation voltages (can also be seen in Figure 15).

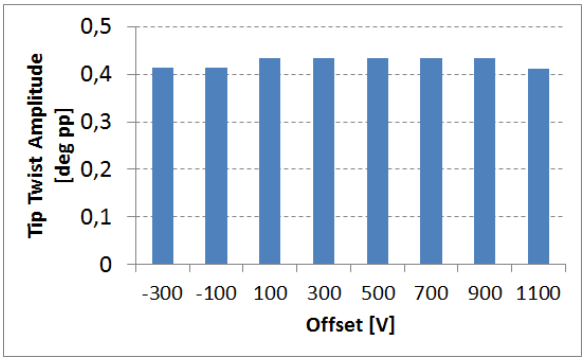

Figure 12: Sweep of Actuation Offset

6.3 Influence of amplitudes

A second study aimed for the influence of the size of the electrical actuator input. Measurements with constant DC offset of 350V, 1Hz frequency and varying amplitudes were carried out. The results can be found in Figure 13. The nonlinearity of the system is obvious. In order to capture the nonlinearity, the influence of the amplitude in dependency of the applied voltage is investigated (see Figure 14). This value is somewhat related to the piezoelectric constant d_{33} which is known from isolated actuators. It becomes obvious, that this value is linearly dependent on the applied amplitude. This relation will help to model the actuation of an active twist excitation more accurately.

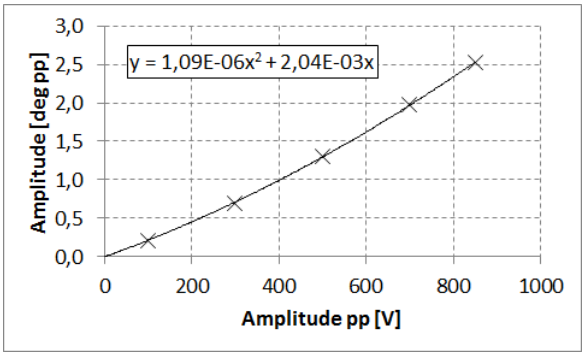

Figure 13: Amplitude sweep

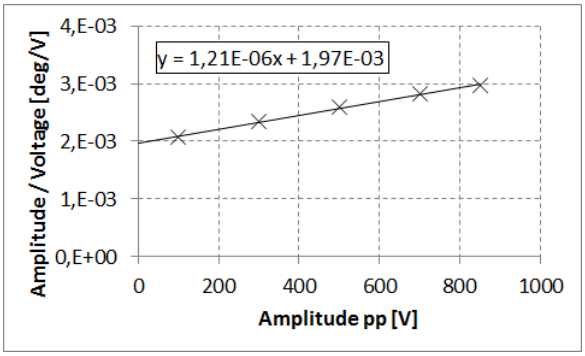

Figure 14: ”Piezoconstant” for the complete blade

6.4 Influence of Very Low Frequencies

A measurement of the dependency of the frequency for very low frequencies was carried out for the AT4 blade. From a structural dynamics point of view there should not be any influences, since inertia is not an issue for frequencies below 6 Hz. At 10 Hz a flapping frequency was excited. In the past there was an observation that the amplitude might increase with decreasing frequency. The Voltage range was kept constant at -500 Volt to +1200 Volt (see Figure 15). It can be clearly seen, that the amplitudes, that are reached do actually increase significantly with decreasing frequency. For higher frequencies, the amplitudes will eventually reach a constant value. This can be clearly seen in Figure 16. The increase compared to the constant value at 6 to 8 Hz was higher than 30 %. This has to be taken into account, when standardizing measurements just as ”quasi static measuements”. The frequency is a very important factor to keep constant. More details of this measuement can be found in

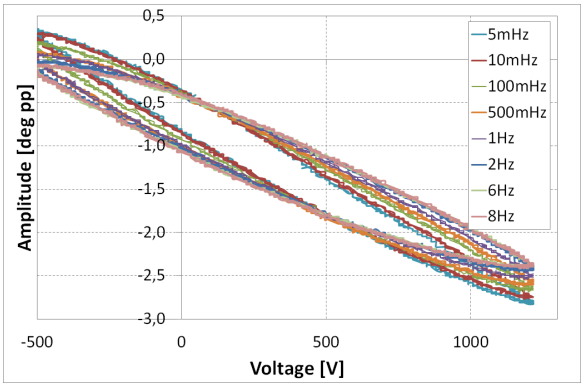

Figure 15: Hysteresis of actuation at different frequencies

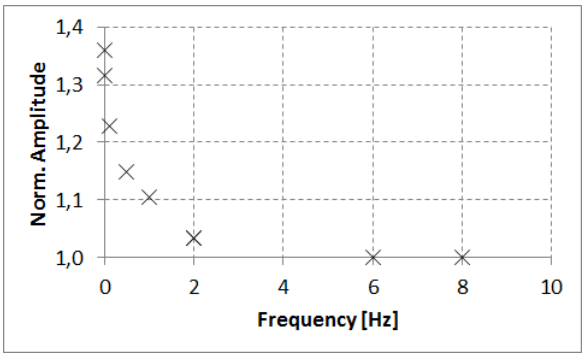

Figure 16: Result of Frequency Sweep

Figure 17 in the appendix.

7 Conclusions

In this paper a methodology to investigate elastic and mass related properties of model rotor blades experimentally in a lab test. The application of these techniques to characterize active twist model rotor blades was demonstrated, but these techniques can be even used for the characterization of passive model rotor blades.

Finally a close look on the nonlinearity of the twist actuation of active twist blades was presented. The limitations of linear modeling were shown, when amplitudes change and actuation frequencies decrease below a few Herz. These findings have to be considered, when the actuation of active twist blades is being modeled.

8 Appendix

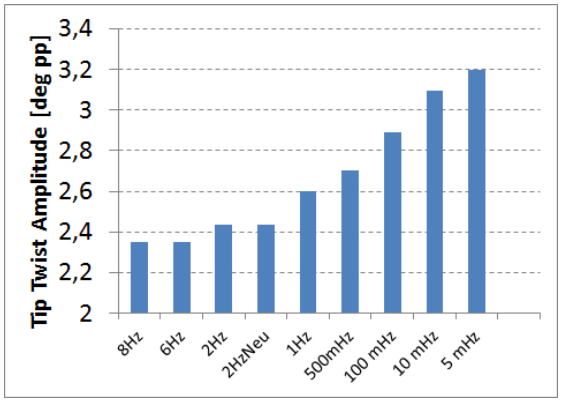

Figure 17: Result of Frequency Sweep

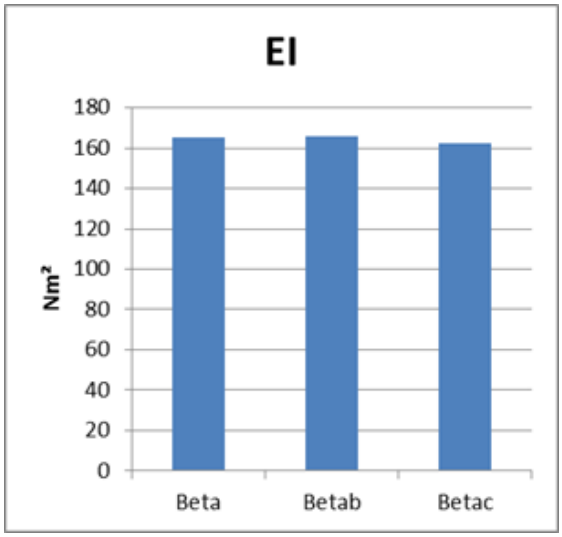

Figure 18: Repeatability of Flap Bending Stiffness

References

[1] Christoph K. Maucher, Boris A. Grohmann, and Peter Jnker. Review of adaptive helicopter rotor blade actuation concepts. In *Adaptronic Congress*. Adaptronic Congress, 2006.

[2] Hans P. Monner, Steffen Opitz, Johannes Riemenschneider, and Peter Wierach. Evolution of active twist rotor designs at dlr. In *AIAA/ASME/AHS Adaptive Structures Conference, Schaumburg, IL, USA*, 2008.

[3] Hans P. Monner, Johannes Riemenschneider, Steffen Opitz, and Martin Schulz. Development of active twist rotors at the german aerospace center (dlr). In *AIAA/ASME/AHS Adaptive Structures Conference, Denver, CO, USA*, 2011.

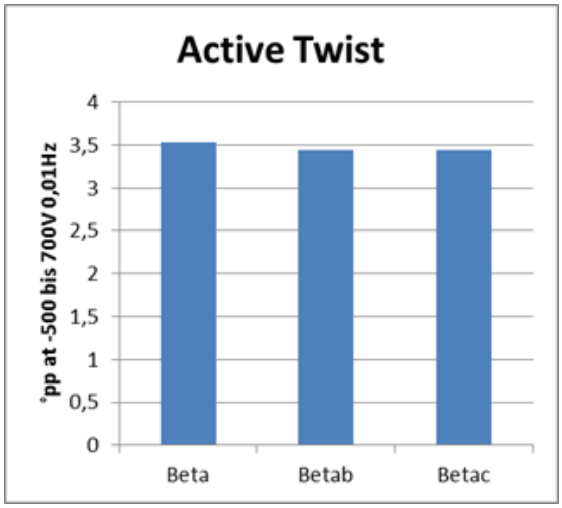

Figure 19: Mass of the STAR blades

[4] Peter Wierach, Johannes Riemenschneider, Steffen Opitz, and Frauke Hoffmann. Experimental investigation of an active twist model rotor blade under centrifugal loads. In *33rd EUROPEAN ROTORCRAFT FORUM*, Kazan, Russia, 2007.

[5] J. Riemenschneider, P. Wierach, and S. Keye. Preliminary study on structural properties of active twist blades. Friedrichshafen, ERF 2003, Sep 2003. Friedrichshafen, ERF 2003, 29th European Rotorcraft Forum.

[6] M. Schulz, S. Opitz, and J. Riemenschneider. A new concept to determine the mass distribution of an active twist rotor blade. *CEAS Aeronautical Journal*, 3(2):117–123, 2012.

COPYRIGHT STATEMENT